IOP Conference Series: Materials Science and Engineering

PAPER • OPEN ACCESS

Modeling, simulation and controller design for a typical bent axis electrohydraulic servo motor

To cite this article: M A Yousef *et al* 2021 *IOP Conf. Ser.: Mater. Sci. Eng.* **1172** 012038

Modeling, simulation and controller design for a typical bent axis electrohydraulic servo motor

M A Yousef[1], M El-Sanabawy[1], G Rabie[2] and R A Rateb[3]

[1] Department of Rockets, Military Technical College, Cairo, Egypt.
[2] Modern Academy for Engineering and Technology, Cairo, Egypt.
[3] Egyptian Armed Forces, Cairo, Egypt.

E-mail: mohamed_abdelwahab@mtc.edu.eg

Abstract. Bent axis electrohydraulic servo motors are one of the Electrohydraulic Servo Motors (EHSMs) family which are used in high frequency, speed, and precision applications such as aerospace applications as well as many military weapon system applications. Therefore, it is essential to understand how such motors affect the whole performance of the system which makes modeling of these motors is an important task to be achieved. Once an accurate model is obtained, an optimum controller can be applied. This paper introduces detailed mathematical modeling of a typical bent axis (EHSM). MATLAB SIMULINK package is used to simulate and control such (EHSM) using PID controller. The PID controller gains were tuned using PD-PI controller to obtain the precision response for the (EHSM). The validity of mathematical modeling was reviewed through some practical experiments.

1. Introduction

Electro-hydraulic Servo Motors (EHSMs) are used in industries where high power to weight ratios, rapid responses, and high precision are needed such as aerospace applications.(EHSMs) motors are used to convert the hydraulic power into mechanical one [1]. They combine the advantages of the hydraulic and electric powers, as they are composed of a hydraulic motor and an electro-hydraulic servo valve (EHSV) respectively[2].

The importance of such devices in recent industries makes their mathematical modeling an important task to be achieved. In the process of designing a new model for a system or improving an existing one, an exact model must be identified [3]. The output of a system can be accurately predicted with good mathematical modeling [4]. So, when the system is well defined, the mathematical model representing this system can be achieved using for example differential equations. These differential equations can be simulated using simulation programs such as the one used in[5].

The point of building a mathematical model is to identify the dynamic behavior of the system besides the ability to control such systems without overshoot or delay through a control action applied in an optimum way to ensure control stability. As it’s known, mathematical modeling of a system is achieved by a huge amount of dependent differential equations that describe every component in the system. Besides the equations that express how these components are related to

The dynamic behavior of an Electro-hydraulic servo system (EHSS) was examined by Attila. The dynamic behavior was investigated using a step response for a non-linear mathematical model. The results showed that the servo valve rapidly followed the valve control signal [6]. Dechrit and Nitin achieved modeling and simulation of a non-linear high-speed servo system used in the operation of a mini-press machine. They built a mathematical model using MATLAB Simulink and the simulation results were tested using experimental system identification which showed the effectiveness of their model [5]. Also, J. Das et al derived a physical nonlinear model for an electrohydraulic actuator. To obtain the actuator dynamics, MATLAB / SIMULINK program was used. The model was validated through experimental work. They focused, experimentally, on the actuator friction and proportional valve characteristics to get closure of the physical model. They tested their model and then a PID controller was introduced to the model. The gain values were found to be suitable and hence providing stable results[7].

Once a good model is obtained an optimum controller can be achieved. PID controller is the most applicable controller used in the industry because of its simplicity in structure and satisfying performance in the industrial process. However, the optimum performance of the PID controller is dependent on three gain values K_P, K_I, K_D proportional, integral, and derivative gains respectively. Tuning of these gain values becomes an essential task to be achieved in order to get a precision performance of such PID controller[3][8]. T. G. Ling et al applied a PID controller to their model to achieve an accurate position tracking of an electrohydraulic actuator. They compared their simulation results with real work, and they concluded that the system with the controller achieved position tracking with high accuracy [9]. There are several types of PID tuning. R. Sen et al applied three types of tuning the PID controller to obtain a precision Positioning of a multi-axis machine[10]. The PD-PI controller is considered an extension of the classical PID controller[11]. Galal A. Hassaan achieved tuning for the classical PID controller using a PD-PI controller to a first-order time-delayed process. The PD-PI controller was compared to the classical PID controller. The results showed that it has a better response than the classical PID controller[12]. Also, Akram F. Singer used the PD-PI controller for tuning the classical PID controller. The proposed controller was applied to a third-order oscillating process. The results showed that the proposed controller has a better performance than the classical PID controller[13].

2. System description

Fig. (1) shows the construction of the considered hydraulic system.

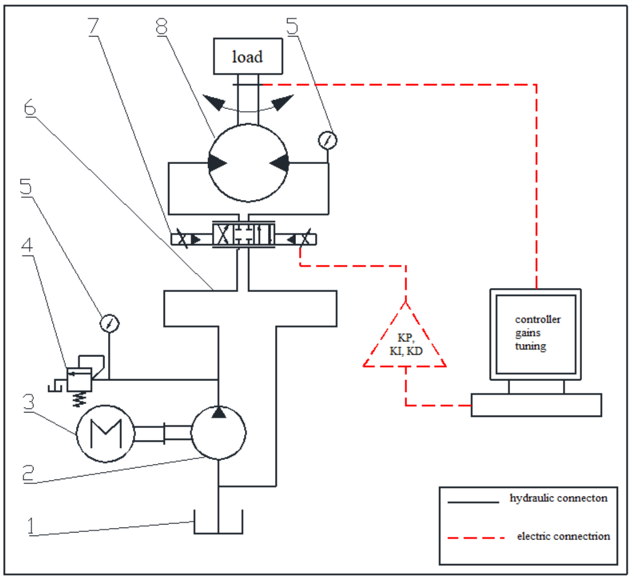

1. open tank 2. Fixed displacement pump 3. Electric motor 4. Relieve valve 5. Pressure -gauges 6. Hydraulic pipelines 7. EHSV 8. Hydraulic motor

Figure 1. System description

2.1 Hydraulic power supply.

2.1.1 construction and operation. The considered hydraulic system is illustrated in fig. (1). It consists of a hydraulic power supply to ensure a constant and controllable supply pressure (Ps). The hydraulic power supply (HPS) is composed of an electric motor (3), [3-phase power electric motor 10 HP and 380 Volt], coupled to (2) a hydraulic fixed displacement gear pump, [533/rev], immersed in (1) a tank, [250 liters]. The supply pressure Ps is limited by (4) a regulated pilot-operated relief valve.

2.1.2 mathematical modeling. The mathematical relations describing the (HPS) , from equation (1) to (20) in [14], have been used to develop a Simulink program .the calculated transient response of the system pressure is plotted Fig.(2).

2.1.3 simulation and results. The following figure shows that the exit pressure ranges from (90.5) bar in the case of throttle area equal to (Ath = 1e-6 m2) which gives a flow rate of (10) l/ min equal to the maximum flow rate of the electro-hydraulic servo valve (EHSV) to (91.4) bar at (Ath = 0) which equates to zero servo valve flow rate. This result shows that the maximum pressure variation is within (1.2%). Therefore, in this study, the HPS pressure is assumed to be constant.

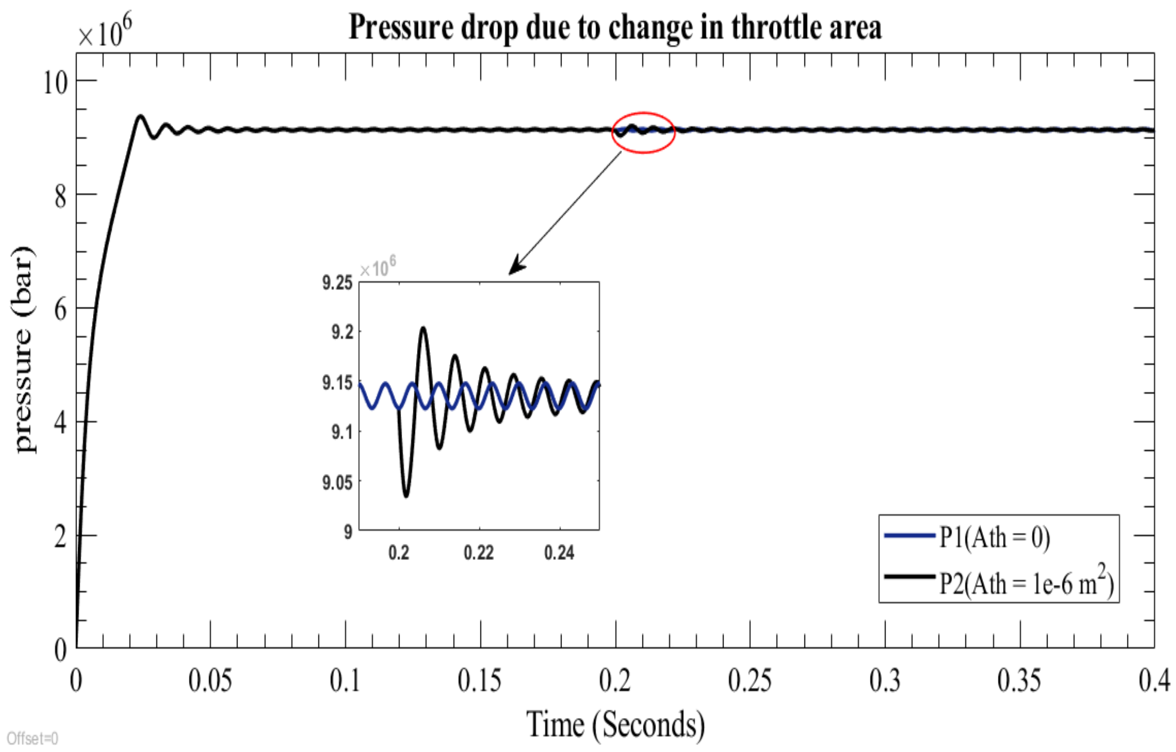

Figure 2. HPS exit pressure at throttle area (Ath= 0 & 1e-6 m2).

2.2 Electro-hydraulic servo valve.

2.2.1 Construction and operation. The (HPS) fluid is controlled by a two-stage electro-hydraulic servo valve (EHSV) of type [MOOG] numbered in fig. (1) by (7). The construction drawing of two-stage EHSV identified by complete parameters is shown in fig. (3). The typical two-stage EHSV receives the pressurized hydraulic fluid that comes from a hydraulic pump. It then transmits the fluid to a bi-directional hydraulic motor at a pressure that is relative to an electrical signal which it receives. Servo valves can guarantee an accurate control of velocity, position, force, and pressure with good damping characteristics.

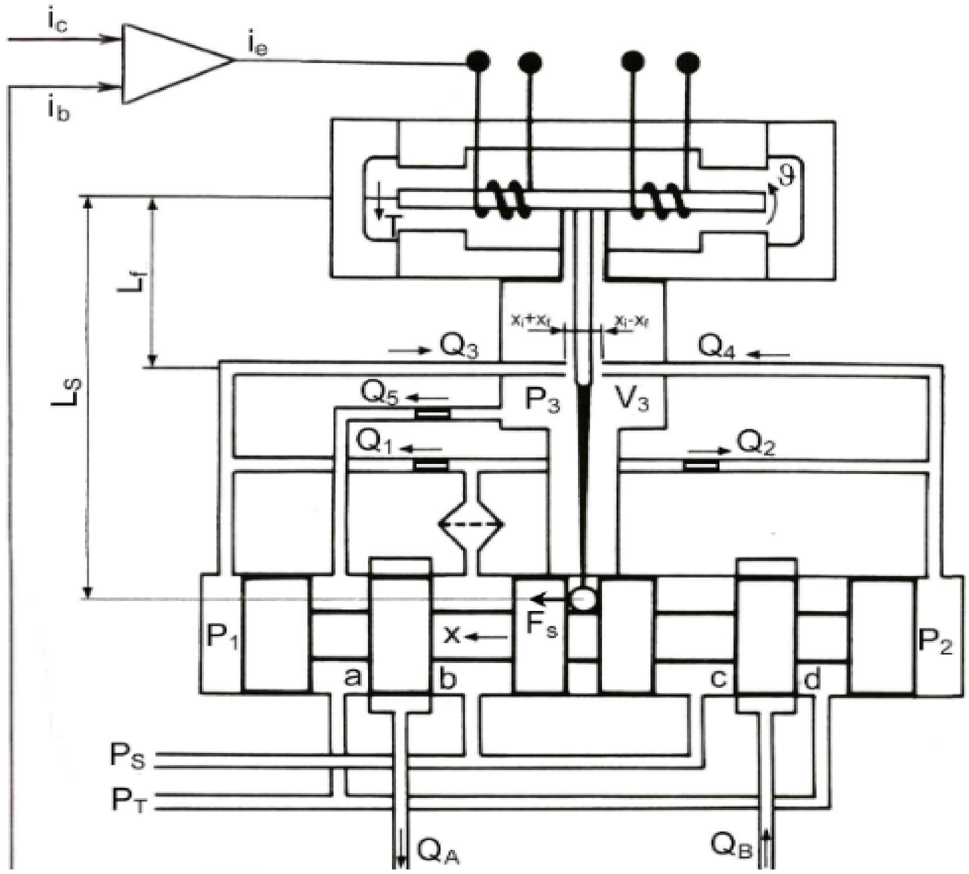

Figure 3. Schematic drawing for two-stage EHSV

2.2.2 Mathematical modeling. The mathematical modeling of the EHSV was developed through equations 1 to 18[2]. The author has partially contribution on the modeling of the two-stage EHSV. The mathematical modeling was developed as follows.

- *Torque motor*

The function of the electromagnetic torque motor is to convert the electric input which is a current of low value within 10 mA into mechanical torque. Neglecting the magnetic hysteresis effect, the equation of the torque motor can be expressed as flows:

$$T = K_i i_e + K_\theta \theta \tag{1}$$

- *Armature dynamics*

The rotating armature movement is illustrated in equations (2) & (3)

$$T = J\frac{d^2\theta}{dt^2} + f_\vartheta \frac{d\theta}{dt} + K_T\theta + T_L + T_P + T_F \tag{2}$$

$$T_p = \frac{\pi}{4} d_f^2 (P_2 - P_1) L_f \tag{3}$$

- *Feedback Torque*

The magnitude of the feedback torque depends on the displacement of the spool and the rotation of the flapper angle which can be described from equation (4) to equation (6)

$$T_F = F_S L_S \tag{4}$$

IOP Conf. Series: Materials Science and Engineering 1172 (2021) 012038 doi:10.1088/1757-899X/1172/1/012038

$$F_S = K_S(L_S\theta + x) \tag{5}$$
$$T_F = F_S L_S = K_S(L_S\theta + x)L_S \tag{6}$$

- *Flapper Position Limiter*

The flapper displacement is restricted by the jet nozzles. Once the flapper limiter reaching one side of the nozzle, a counter torque is produced which can be expressed in equation (7):

$$T_L = \begin{cases} 0 & |x_f| < x_{fL} \\ R_f \dfrac{d\theta}{dt} - (|x_f| - x_{fL})K_L L_f sign(\theta) & |x_f| > x_{fL} \end{cases} \tag{7}$$

- *Flow rates and the restriction areas of the flapper valve*

1. *Flow rates*

The equations of the flow rates can be expressed in equations (8) to (13).

$$Q_1 = C_d A_o \sqrt{\frac{2}{\rho}(P_s - P_1)} = C_{12}\sqrt{(P_s - P_1)} \tag{8}$$
$$Q_2 = C_d A_o \sqrt{\frac{2}{\rho}(P_s - P_2)} = C_{12}\sqrt{P_s - P_2} \tag{9}$$
$$Q_3 = C_d \pi d_f (x_i + x_f)\sqrt{\frac{2}{\rho}(P_1 - P_3)} = C_{34}(x_i + x_f)\sqrt{(P_1 - P_3)} \tag{10}$$
$$Q_4 = C_d \pi d_f (x_i - x_f)\sqrt{\frac{2}{\rho}(P_2 - P_3)} = C_{34}(x_i - x_f)\sqrt{(P_2 - P_3)} \tag{11}$$
$$Q_5 = C_d A_s \sqrt{\frac{2}{\rho}(P_3 - P_T)} = C_5\sqrt{(P_3 - P_T)} \tag{12}$$
$$x_f = L_f\theta \tag{13}$$

2. *Restricting areas*

The modeling of the restricting areas of the flapper valve are shown in equations (14) & (15).

$$\left.\begin{aligned} A_a = A_c = \omega c \\ A_b = A_d = \omega\sqrt{(x^2 + c^2)} \end{aligned}\right\} \quad For\ x \geq 0 \tag{14}$$

$$\left.\begin{aligned} A_a = A_c = \omega\sqrt{(x^2 + c^2)} \\ A_b = A_d = \omega c \end{aligned}\right\} \quad For\ x \leq 0 \tag{15}$$

3. *Continuity equations applied to flapper valve chambers.*

If the continuity equation is applied to the flapper champers, equation (16) to (18) will be introduced.

$$Q_{ba} = Q_1 - Q_3 + A_s\frac{dx}{dt} = \frac{d}{dt}\left(\frac{V_o - A_s x}{B}P_1\right) \tag{16}$$
$$Q_{dc} = Q_2 - Q_4 - A_s\frac{dx}{dt} = \frac{d}{dt}\left(\frac{V_o + A_s x}{B}P_2\right) \tag{17}$$
$$Q_3 + Q_4 - Q_5 = \frac{d}{dt}\left(\frac{V_3}{B}P_3\right) \tag{18}$$

These mathematical relations from (1) to (18) were used to develop a computer simulated program (Simulink). Fig. (4,5) show where these numerical values where found.

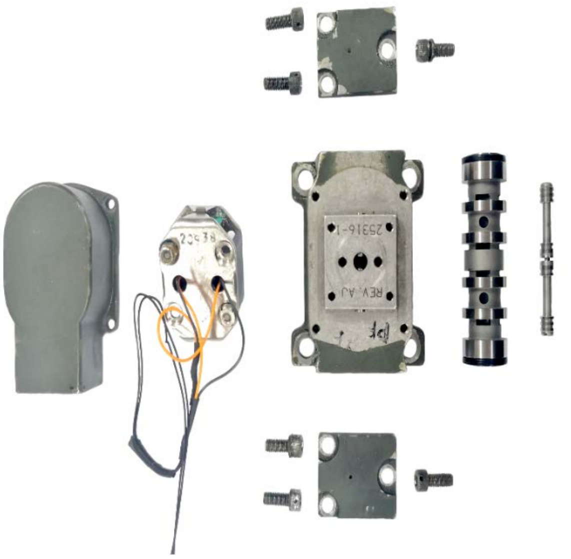

Figure 4. Disassembled two-stage EHSV

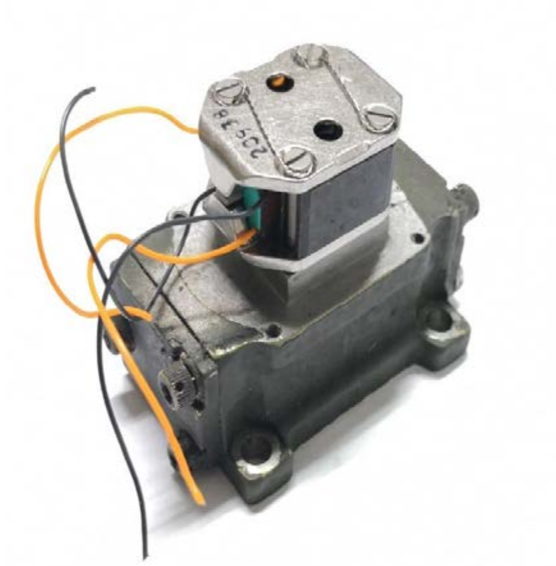

Figure 5. Typical two-stage EHSV

The servo valve is a complicated device that contains a higher order of nonlinear response. To perform an accurate mathematical model, knowledge of a big number of internal parameters is required. These parameters are adjusted together by the manufacture to tune the response of the valve and this information is not available for the users[6]. The previous section illustrates the detailed mathematical modeling of the EHSV.

2.2.3 Simulation and results. The following figure shows the pressure response (P1, P2) at the two sides of the spool. The pressure difference $\Delta P = (P1 - P2)$ is responsible for the movement of the spool. This spool movement generates a flow rate (Q_A, Q_B) which in turn rotates the hydraulic motor.

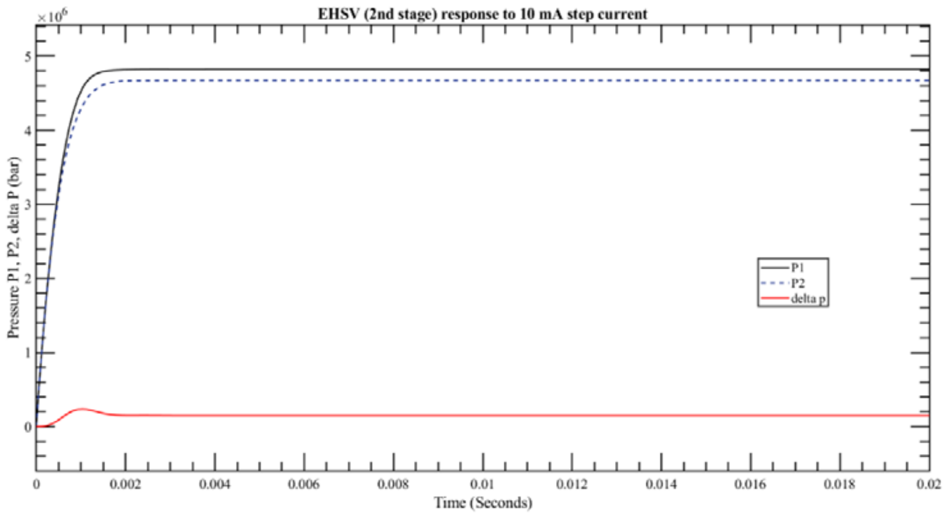

Figure 6. EHSV response to step 10 mA electric current

2.3 Hydraulic motor

2.3.1 Construction and operation. The hydraulic motor is a bent axis responsible for converting the hydraulic fluid pressure into mechanical torque and the hydraulic flow into angular displacement. The hydraulic circuit is provided by pressure gages at the exist of the (HPS) and the entrance of the hydraulic motor as illustrated in fig. (1). The hydraulic motor in concern is illustrated in the fig. (7) consists of a front and rear casing (1,2) port plate (3), cylinder block (4), piston head (5), piston rod assembly (6), bearing set (7) leakage port (8) and output shaft (9). The input flow rate with high pressure (Q_{in}) is supplied to the port plate (3) which transmits the oil to the cylinder block and the piston chamber (4,5). The high-pressure line connected to the piston chambers causes pressure force. This pressure force is resolved at the end of the connecting rod into two components, axial and tangential force. The axial force is sustained by the bearings while the tangential force causes the driving of the hydraulic motor shaft against the loading torque. Hence, the loading torque value depends on the supply (inlet) pressure P_s and hydraulic motor speed is based on the supply (inlet) flow rate Q_{in}. The intake and the drain of the oil flow of the hydraulic motor are controlled by the port plate (3).

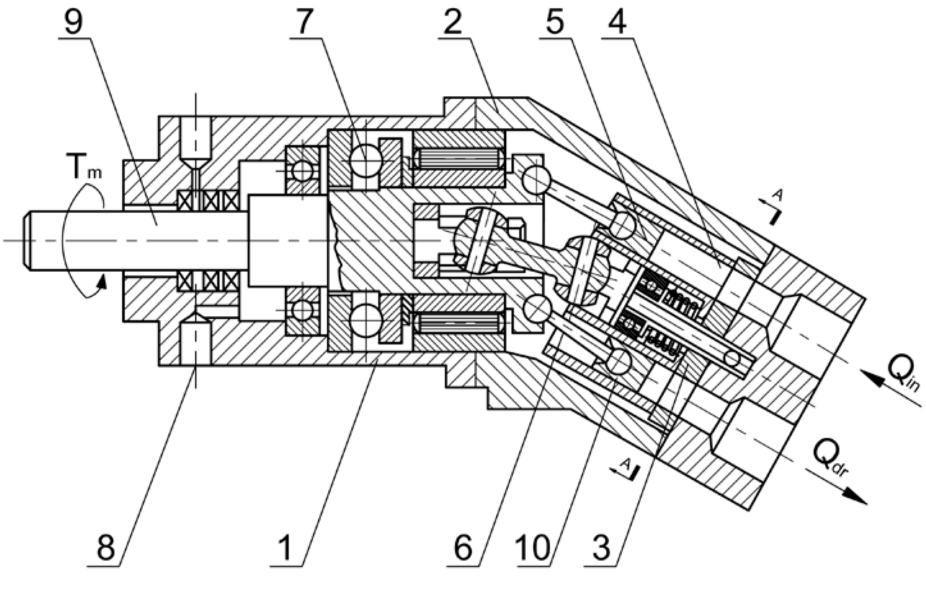

Figure 7. Schematic drawing for the hydraulic motor.

2.3.2 Mathematical modeling

The inlet (intake) and outlet (drain) flow rates can be calculated from the following equations:

$$Q_{ini}= C_d A_{ini} \sqrt{\frac{2}{\rho}(P_s\text{-}P_{ci})} \tag{19}$$

$$Q_{dri}= C_d A_{dri} \sqrt{\frac{2}{\rho}(P_{ci}\text{-}P_T)} \tag{20}$$

$$Q_{in}= \sum_{1}^{i} Q_{ini} \tag{21}$$

$$Q_{dr}=\sum_{1}^{i} Q_{dri} \tag{22}$$

The following equation results from applying the continuity equation to the individual cylindrical chamber of the hydraulic motor taking into consideration the volume variation of the chamber and internal leakage.

$$Q_{ini}\text{-}Q_{dri}\text{-}\frac{dx_i}{dt}A_S\text{-}\frac{P_{ci}}{R_i}=\frac{V_{ci}+X_iA_S}{B}\frac{dP_{ci}}{dt} \tag{23}$$

$$A_S=\frac{\pi}{4}d_8^2 \tag{24}$$

$$V_{ci}=A_S\,L_C \tag{25}$$

The piston displacement can be expressed as a function of rotational angle as follows:

$$X_i=\frac{Y_i}{sin\propto}=\frac{d_7(1\text{-}cos\theta_{mi})}{2\,sin\propto} \tag{26}$$

The torque on one piston of the hydraulic motor is calculated as follows:

$$T_{mi}=\frac{d_7}{2}P_{ci}A_S\,sin\propto sin\theta_{mi} \tag{27}$$

Hence, the total torque (motor torque) can be expressed as:

$$T_m=\sum_{1}^{i} T_{mi} \tag{28}$$

And then the equation of motion of port plate under the action of motor torque can be expressed as follows:

$$T_m=J\ddot{\theta}_{mi}+f\dot{\theta}_{mi}+T_L \tag{29}$$

Equations from (18) to (29) were used to develop a Simulink program for the hydraulic motor[16]. Fig. (8) shows where these numerical values were found.

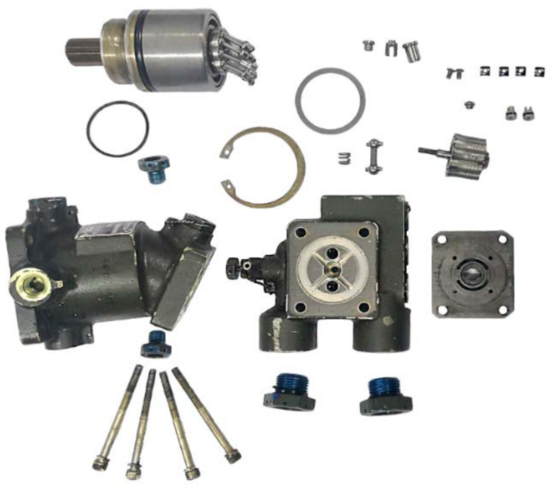

Figure 8. Disassembled hydraulic motor.

IOP Conf. Series: Materials Science and Engineering 1172 (2021) 012038 doi:10.1088/1757-899X/1172/1/012038

2.3.3 Simulation and results. The hydraulic motor was connected directly to the HPS and the response of the hydraulic motor angular velocity was illustrated in fig. (9).

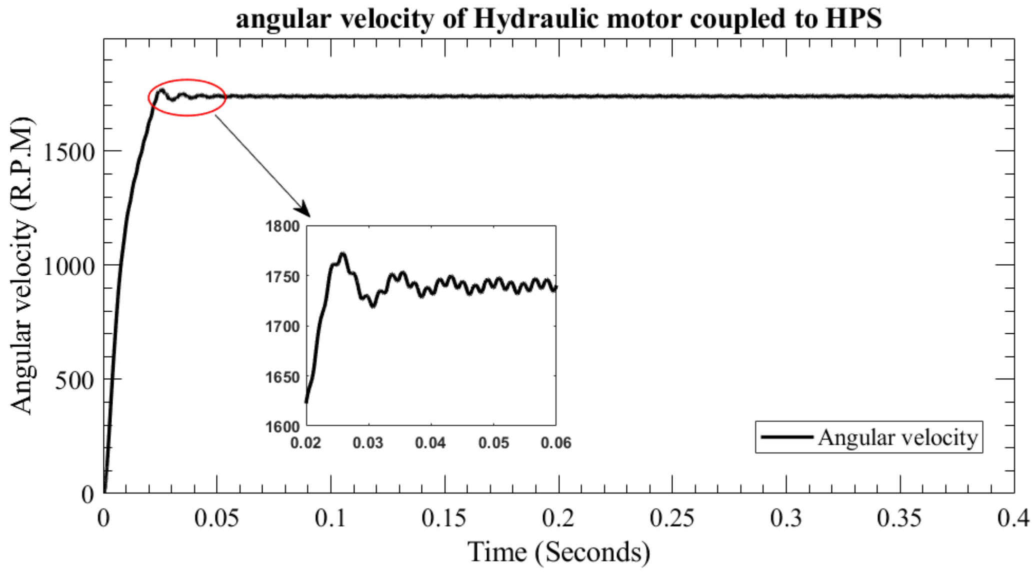

Figure 9. Hydraulic motor angular velocity response to step throttle area Ath = 1e-6 m2.

2.4 Electro-hydraulic servo motor (EHSM)

2.4.1 Construction and operation. The motor understudy shown in fig. (10) is a bent axis electrohydraulic servo motor used in the rocket launcher system. The function of this motor is the movement of the rocket system in vertical and longitudinal planes. Once the guidance commands reach the control panel of the rocket launcher, they are automatically transformed into electrical signals to the EHSV which in turn rotate the hydraulic motor at an angle that corresponds to the guidance signal. It composes 9 pistons to reduce the pulsation of the supplied pressure. The operating ranges of frequency and power for this motor are much higher compared with other applications. The operating pressure is 3000 psig i.e about 200 bar.

Figure 10. Typical electro-hydraulic servo motor.

2.4.2 Mathematical modeling. The EHSV was simulated through equation (1) to (18), moreover, the hydraulic motor was simulated through equations from (19) to (29). The continuity equations describing the room (chamber) between the EHSV and the hydraulic motor are as follows:

$$\sum_{1}^{i} Q_{ini} - Q_A = \frac{d}{dt}\left(\frac{V_o}{B} P_{ba}\right) \tag{30}$$

$$Q_{ba} - \sum_{1}^{i} Q_B = \frac{d}{dt}\left(\frac{V_o}{B} P_{dc}\right) \tag{31}$$

Fig. (11) shows the the schematic drawing for the EHSM.

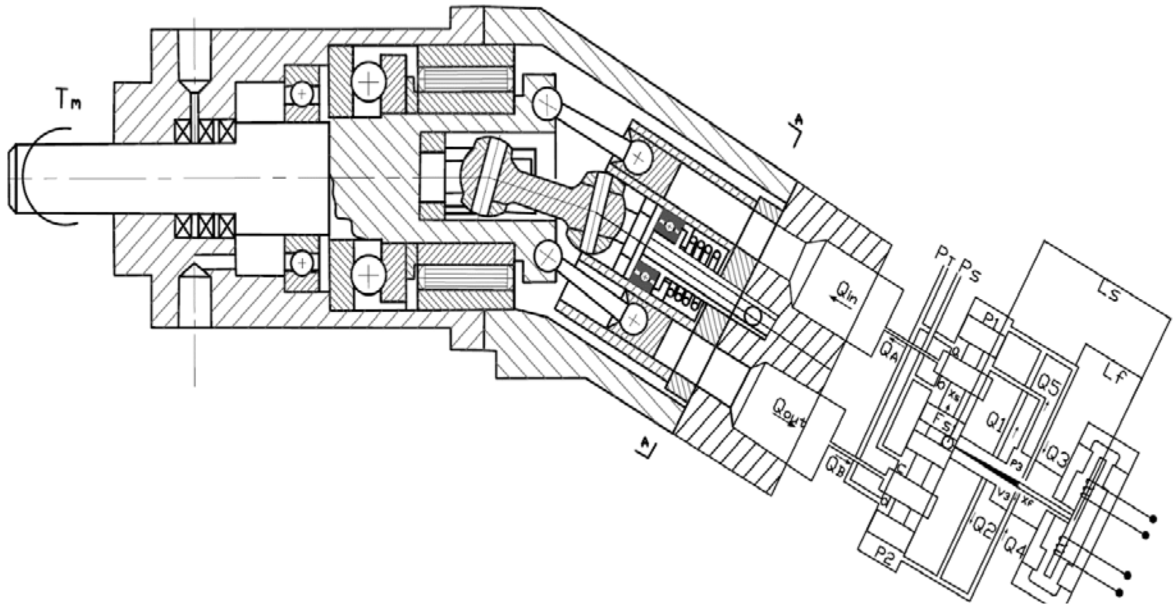

Figure 11. Schematic drawing for the EHSM

The hydraulic motor was mathematically modeled through equations from (1) to equation (31). MATLAB Simulink program was used to simulate these equations. Figure (12) shows the constructed program block veiw.

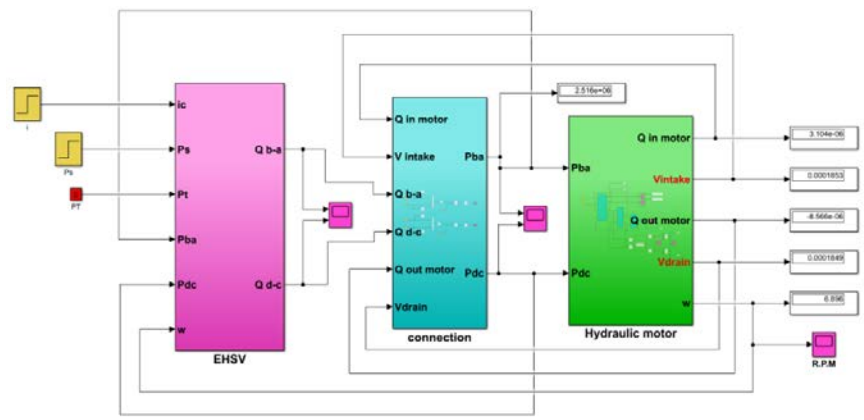

Figure 12. Simulink Program Block View.

2.4.3 Simulation and results. Figure (13) shows the dynamic behavior response of the EHSM to 10 mA electric current input to the EHSV.

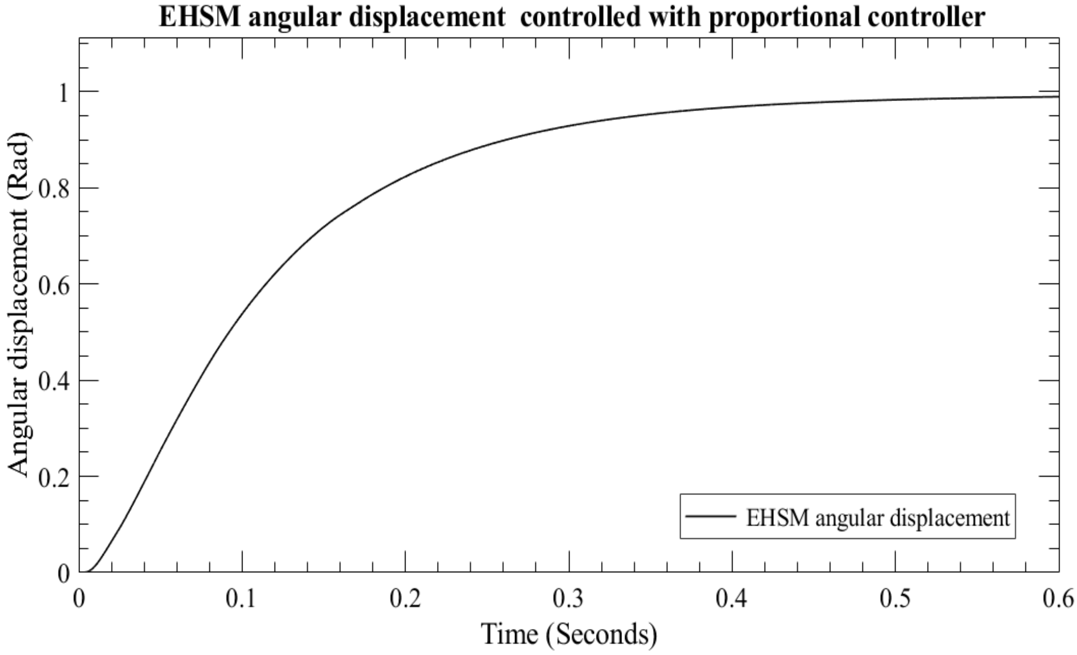

Figure 13. EHSM angular displacement response to 10 mA electric current input.

3. PID controller design

MATLAB Simulink program is also used for designing the PID controller with preliminary gain parameters (K_P, K_I, and K_D) based on trial and error of the model. The best values of controller gains were found to be Kp = 21, Ki = 5 , and Kd = 0. Fig.(14) shows the model response for the controlled EHSM compared to the EHSM.

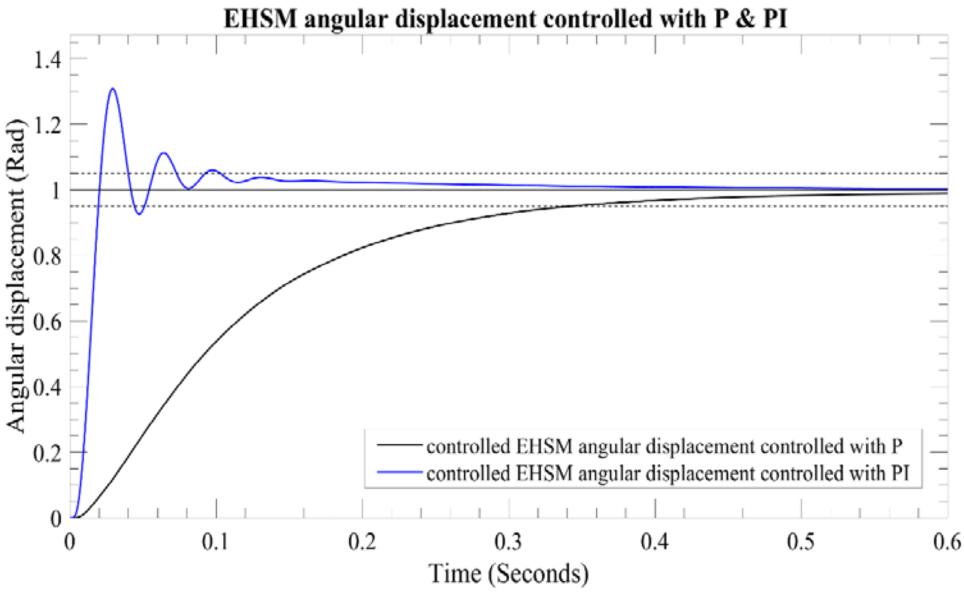

Figure 14. EHSM angular displacement response to 10 mA electric current step input.

4. PD-PI controller design

The proposed controller is a proportional- derivative (PD) proportional - integral (PI) controller. The two parts of the controller (PD-PI) are connected in series as shown in figure (15). The system error is the input of the first part and its output is the input of the second part [11], [12], [13], [17].

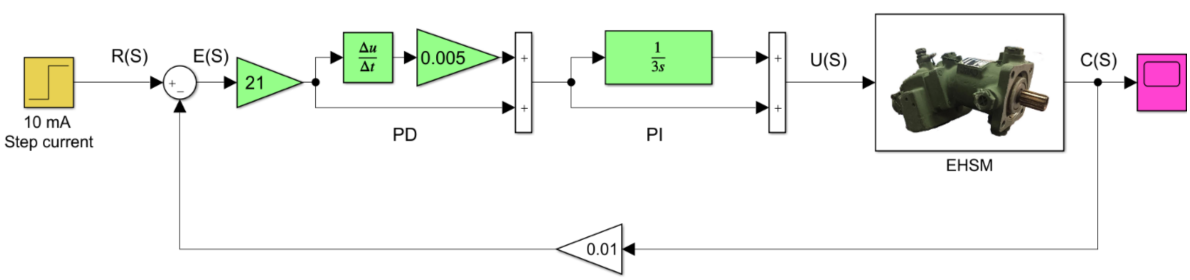

Figure 15. Construction of PD-PI controller.

The following figure shows the response of the PD-PI controller with respect to the classical PID controller.

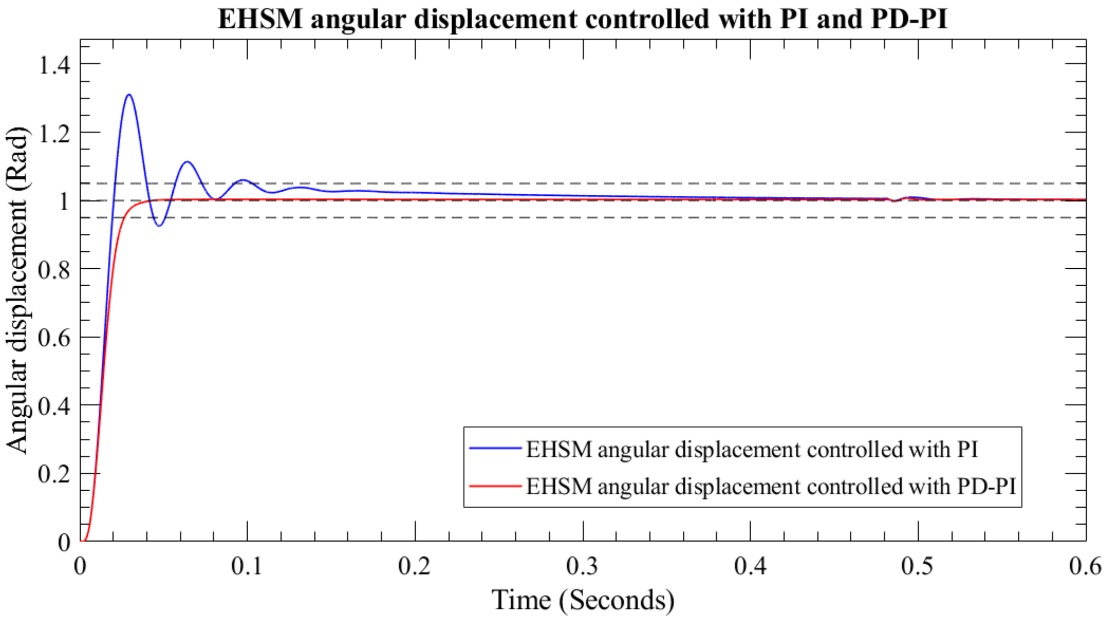

Figure 15. EHSM angular displacement controlled with PID and PD-PI.

5. Validation

The following figure shows that the more pressure you apply, the higher slope you will get. This can be explained by the nonlinearity of the model. As the model pressure is increased, the model becomes more sensitive to the input signal which increases the velocity with a small value of current.

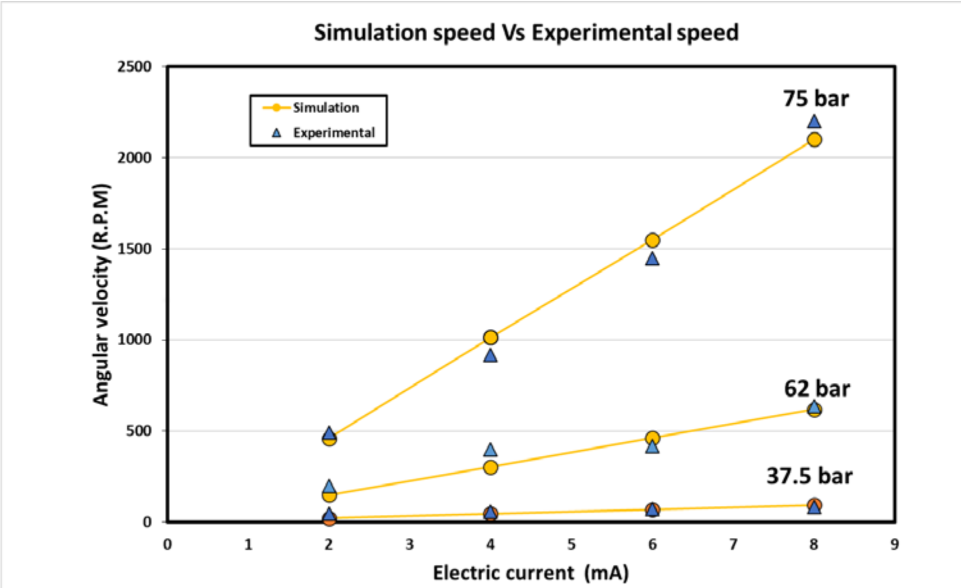

Figure. 17 Experimental and simulation results of the EHSM for different supply pressures and input current.

6. Conclusion

A complete modeling for a typical bent axis electro-hydraulic servo motor was done. MATLAB/ Simulink program was used to achieve the model. A new generation for the classical PID controller (PD-PI) was applied to the model. The model was validated through some exprementatal work.

Nomenclature

B	Bulk modulus of oil	=	1.5e9	(Pa)
c	Radial clearance			(m)
d_5	Diameter of return orifice N5 d5(m)	=	0.0006	(m)
d_f	flapper diameter	=	0.0005	(m)
d_{fn}	Hydraulic amplifier nozzles N1 & N2 diameter	=	0.0005	(m)
d_s	Spool diameter	=	0.0046	(m)
F_s	Spool Damping coefficient	=	2	(Ns/m)
f_{th}	Armature damping coefficient	=	0.002	(Nms/rad)
J	Moment of inertia of the rotor	=	5e-7	(Nms^2)
K_i	Current gain	=	0.556	
K_{Lf}	Flapper seat equivalent stiffness	=	5e6	(N/m)
K_s	Feedback spring stiffness	=	900	(N/m)
K_T	Flexible tube rotational stiffness	=	10	(N.m/rad)
K_{th}	Armature rotational angle torque gain	=	9.45e-4	
L_f	Flapper length	=	0.009	(m)
L_s	Mechanical feedback spring length	=	0.03	(m)
M_s	Spool mass	=	0.02	(kg)
P_{c1} & P_{c2}	Hydraulic motor pressures			(Pa)
P_T	Return Pressure	=	0	(Pa)

IOP Conf. Series: Materials Science and Engineering 1172 (2021) 012038 doi:10.1088/1757-899X/1172/1/012038

Q1	Flow rate in the left orifice			(m3/s)
Q2	Flow rate in the right orifice			(m3/s)
Q3	Left flapper nozzle flow rate			(m3/s)
Q4	Right flapper nozzle flow rate			(m3/s)
Q5	Flapper valve drain flow rate			(m3/s)
R_f	Equivalent flapper seat material damping coefficient	=	5000	(Nsm)
V_3	Initial Volume of oil in the return chamber	=	5e-6	(m^3)
V_o	Initial volume of oil in spool side chamber	=	2e-6	(m^3)
Xi	Flapper limiting displacement	=	30e-6	(m)
π	Pi	=	3.14159	
ρ	Oil density	=	867	(Kg/m^3)
ω	Ports width on the valve sleeve			(m)

References

[1] Merritt H *1967. Hydraulic Control Systems.* New York: Wiley.
[2] Rabie M *2009. Fluid Power Engineering*. New York: McGraw-Hill.
[3] Ogata K 2*016. Modern Control Engineering.* (Delhi): Pearson.
[4] Ljung L *1999 Wiley Encyclopaedia of Electrical and Electronics Engineering* 29 3026
[5] Maneetham D and Afzulpurkar N 2010 Modeling, Simulation and Control of High Speed 4
[6] Kővári A 2015 Mathematical Model and Simulation of Electrohydraulic Servo Systems *Tudomány Hete a Dunaújvárosi Főiskolán* 2009.
[7] Santosh J, Mishra K et al 2017 Nonlinear Modeling And PID Control Through Experimental Characterization for an Electrohydraulic Actuation System *J. Brazilian Soc. Mech. Sci. Eng.* **39** 1177.
[8] Dorf R and Bishop R *2011 Modern control systems* 12th ed New Jersey: Pearson.
[9] Ling T, Rahmat M et al 2012 System Identification and Control of an Electro- Hydraulic Actuator System *2012 IEEE 8th International Colloquium on Signal Processing and its Applications*.
[10] Sen R, Pati C et al 2014 Comparison Between Three Tuning Methods of PID Control for High Precision Positioning Stage *J. Metrol. Soc. India* **30**
[11] Atherton D 2016 PI-PD, an Extension of Proportional-Integral-Derivative Control *Measurement and Control* **49** 161 (United Kingdom).
[12] Hassaan G 2014 Tuning of a PD-controller used with Second Order Processes *International Journal of Engineering Research & Technology (IJERT)***3** 120.
[13] Singer A, Hassaan G, et al 2020 Tuning Of a PD-PI Controller Used with a Third Order Process *International Journal of Engineering Research & Technology (IJERT)* **9** 6.
[14] Rabie M 1991 Dynamic Performance of Pilot operated Hydraulic Relief Valves *International Conference on Aerospace Sciences & Aviation Technolog* **4** 135 (cairo).
[15] Automatisés S, Fadel M, et al 2019 Modeling, Simulation and Control of a Fly-by-wire Flight Control System Using Classical PID and Modified PI-D Controllers **52** 267.
[16] Sallam A, Rabie M et al 2009 Dynamic Behaviour of a Hydraulic Motor Controlled by a Poppet Type Directional Control Valve International Conference on *Aerospace Sciences & Aviation Technolog* **13** 1 (Cairo).
[17] Singer A, Hassaan G, et al 2020 Robustness of PI-PD Controller Used with Third Order Processes *International Journal of Engineering and Techniques* **6** 4.